FTUV/95-67
IFIC/95-70
March 1996

Dynamical $\mathcal{O}(\alpha)$ Effects in Forward-Backward Asymmetries of Heavy Quarks

Michael M. Tung *

Departament de Física Teòrica, Universitat de València
and IFIC, Centre Mixte Universitat València — CSIC,
C/ Dr. Moliner, 50, E-46100 Burjassot (València), Spain.

ABSTRACT

We examine the $\mathcal{O}(\alpha)$ forward-backward asymmetries for the production process $e^+e^- \to \gamma, Z \to q\bar{q}(g)$, tagging the outgoing heavy-quark jet at center-of-momentum energies off the Z-peak. The complicated analytic results are reduced to simple polynomial forms that provide excellent approximations. For charm and bottom quark, a full dynamical cancellation gives $\mathcal{O}(\alpha)$ zeros in the forward-backward asymmetry close to the Z-peak. We conclude with a detailed numerical analysis of our results.

PACS number(s): 11.38.Bx, 11.80.Fv, 14.65.-q

*Feodor-Lynen Fellow

The measurement of asymmetries in the production of fermion pairs at e^+e^- colliders has been proven as an indispensable tool to examine rigorously the most important properties of the Standard Model. In general, these experimental techniques have advanced to such an extent that theoretical predictions beyond the Born approximation in the perturbative series of the relevant couplings have to be taken into account in order to agree with the given measurement precision.

Of particular interest is the forward-backward asymmetry A_{FB}^f which results from the vector (V)/axial-vector (A) interference terms of the intermediate γ, Z bosons in the production process $e^+e^- \to \gamma, Z \to f\bar{f}$. Therefore, its measurement allows for a direct determination of the relative strength between the V- and A-components of the fermion coupling to the neutral current, or, equivalently, for a precise determination of the effective electroweak mixing angle $\sin^2\theta_W$. Experiments that measure A_{FB}^f for various quark flavors and leptons are carried out by the different LEP and SLD collaborations.

This work concentrates on dynamical QCD one-loop effects in the forward-backward asymmetries of heavy quarks. For the charm and bottom quark, high-precision measurements on the Z-peak are performed by the ALEPH, DELPHI, and OPAL collaborations at LEP [1,2,3]. In the theoretical literature, a first analytical treatment of massive $\mathcal{O}(\alpha)$ corrections for A_{FB}^q at the Z-peak can be found in an article by Djouadi *et al.* [4]. Only recently their result (given as an expansion in the quark mass) has been slightly corrected by Stav and Olsen [5]. The exact analytical formulas are lengthy and complicated, see *e.g.* Ref. [6].

However, in the following we shall present compact Schwinger representations for the $\mathcal{C}$-odd structure function in the differential production cross section for heavy quarks. To the best of our knowledge no such representations have been treated in the literature before. Subsequently, we use these results to find simple polynomial expressions for the single-jet forward-backward asymmetry including $\mathcal{O}(\alpha)$ radiative corrections. These approximate formulas give very accurate estimates valid over the entire physically relevant energy spectrum, which will then allow us to reveal interesting dynamical properties of A_{FB}^q at QCD one-loop level. Finally, we conclude this work with a detailed numerical analysis for charm-, bottom-, and top-quark production.

For heavy-quark production $e^+e^- \to \gamma, Z \to q\bar{q}$, the differential cross section is usually integrated over the azimuthal angle to yield the following decomposition in terms of the polar angle θ of the scattered quark

$$\frac{d\,\sigma}{d\cos\theta} = \tfrac{3}{8}(1+\cos^2\theta)\,\sigma_{_U} + \tfrac{3}{4}\sin^2\theta\,\sigma_{_L} + \tfrac{3}{4}\cos\theta\,\sigma_{_F}. \tag{1}$$

The structure functions $\sigma_{_U}$ and $\sigma_{_L}$ correspond to unpolarized and longitudinally polarized gauge bosons, respectively, and their sum gives the total cross section $\sigma_{_T} = \sigma_{_U} + \sigma_{_L}$. Clearly, in Eq. (1) the term containing $\sigma_{_F}$ is the only component that changes sign under the replacement $\theta \to \pi - \theta$, and thus constitutes the odd term under charge conjugation $\mathcal{C}$ in the fermionic final state.

At the Born level, $\sigma_{_F}$ is straightforwardly given by

$$\sigma_{_{F/0}} = 8\pi\,\frac{\alpha^2}{q^2}\,v^2 g^{VA}, \tag{2}$$

where q is the momentum transfer carried by the exchanged γ or Z boson, and $v = \sqrt{1-4m^2/q^2}$ with quark mass m. The factor g^{VA} incorporates all couplings that result from the mixed VA interference in the intermediate state

$$g^{VA} = -Q_q a_e a_q\,\mathrm{Re}\,\chi_{_Z} + 2\,v_e a_e v_q a_q |\chi_{_Z}|^2. \tag{3}$$

Here, the fractional charge of the quark is Q_q and the relevant electroweak coulings are $v_f = 2\,T_z^f - 4\,Q_f \sin^2\theta_{_W}$ and $a_f = 2\,T_z^f$ for $f = e, q$. The Z-propagator displays the typical resonance behavior for the decay of an instable massive particle so that we have

$$\chi_{_Z}(q^2) = \frac{g_{_F}\,M_{_Z}^2\,q^2}{q^2 - M_{_Z}^2 + iM_{_Z}\,\Gamma_{_Z}} \quad \text{with} \quad g_{_F} = \frac{G_{_F}}{8\sqrt{2}\,\pi\alpha} \approx 4.299\cdot 10^{-5}\,\mathrm{GeV}^{-2}. \tag{4}$$

The calculation of $\sigma_{_F}$ including first-order corrections in the strong coupling involves the summation of virtual soft-gluon contributions and hard-gluon bremsstrahlung. A closed form expression was derived in Ref. [6]:

$$\sigma_{_{F/1}} = \sigma_{_{F/0}}\left[(1+\mathrm{Re}\,\tilde{A}+\mathrm{Re}\,\tilde{C})\,v + \frac{\alpha_s}{4\pi}\,C_{_F}\,\frac{1}{v}\left\{ -(4-5\xi)\mathcal{S}_2 - \xi(1-\xi)(\tilde{\mathcal{S}}_3+\tilde{\mathcal{S}}_5)\right.\right.$$
$$\left.\left. -2(4-3\xi)\mathcal{S}_4 + \xi\mathcal{S}_6 + 2(\mathcal{S}_8+\mathcal{S}_9+3\mathcal{S}_{10}-\mathcal{S}_{11}) + 2(1-\xi)(2-\xi)\tilde{\mathcal{S}}_{12}\right\}\right], \tag{5}$$

where $C_F = 4/3$ is the usual Casimir operator of the $SU(3)$ color group and an additional mass parameter $\xi = 1 - v^2 = 4m^2/q^2$ has been introduced.

The coefficients $\tilde{A}$ and $\tilde{C}$ are the conventional QCD form factors in the notation of Refs. [6,7] (using the Feynman gauge and on-shell renormalization), and correspond to the gluonic corrections of the V and A currents, respectively. For the axial form factor $\tilde{C}$, it has explicitly been shown that different methods like anticommuting γ_5 within dimensional regularization [8], dimensional reduction [9], and the 't Hooft–Veltman prescription for γ_5 [6] all produce identical results.

In the following, we shall only be interested in the high-energy ($v \to 0$) and low-energy ($v \to 1$) limits of the form factors $\tilde{A}$ and $\tilde{C}$

$$\boxed{v \to 1} \quad \mathrm{Re}\,\tilde{A} \sim \mathrm{Re}\,\tilde{C} \sim \frac{\alpha_s}{4\pi} C_F \Bigg[\ln^2 \xi - (1 + 4\ln 2)\ln\xi + 2(1 + 2\ln 2)\ln 2 + \tfrac{4}{3}\pi^2 - 4 + \mathcal{O}(\xi) \Bigg], \tag{6}$$

$$\boxed{v \to 0} \qquad \mathrm{Re}\,\tilde{A} \sim \frac{\alpha_s}{4\pi} C_F \left[\frac{\pi^2}{v} - 8 + \pi^2 v + \tfrac{2}{9}(1 + 24\ln 2)v^2 + \mathcal{O}() \right], \tag{7}$$

$$\boxed{v \to 0} \qquad \mathrm{Re}\,\tilde{C} \sim \frac{\alpha_s}{4\pi} C_F \left[\frac{\pi^2}{v} - 4 + \pi^2 v - \tfrac{2}{9}(11 - 24\ln 2)v^2 + \mathcal{O}() \right]. \tag{8}$$

Eq. (6) clearly states that for nearly massless quarks or sufficiently high center-of-momentum energies, $E_{cms} = \sqrt{q^2}$, the virtual-gluon corrections become insensitive to the parity property of the relevant vector-boson vertex. However, in the asymptotic energy range near threshold, $\tilde{A}$ and $\tilde{B}$ differ by a finite contribution reflecting the distinct nature of the underlying symmetries. Following the reasoning by Schwinger [10], both $1/v$-poles in Eqs. (7) and (8) correspond to the strong attraction between the color charges (quarks) in the non-relativistic limit with a relative velocity $2v \ll 1$.

In Eq. (6) the collinear IR divergences emerge as logarithmic singularities for $\xi \to 0$, and eventually cancel when the hard-gluon parts are added. (Note that the trivial soft IR divergences have already been neglected as indicated by the wiggle, *viz.* Ref. [6].) The full analytic solutions of the $q\bar{q}g$ phase-space integrals $\mathcal{S}_i$, $i = 2, \ldots, 12$, have been calculated and classified in Ref. [7]. Much simpler results which approximate the exact solutions in

the important high- and low- energy domains were presented in Ref. [11] [†].

It is now straightforward to take the limits in the total expression Eq. (5). For $v \to 1$, we obtain

$$\sigma_{F/1} \sim \sigma_{F/0}\Big[\, 1 + \alpha_s \, \mathcal{O}(\,-\,) \,\Big], \tag{9}$$

i.e. the QCD corrections for σ_F are genuine quark-mass effects and can safely be neglected in the high-energy region. This prediction was already made in Ref. [8]. On the other hand, the asymptotic behavior close to threshold has never before been considered in the literature. Our result for $v \to 0$ is

$$\sigma_{F/1} \sim \sigma_{F/0} \left[1 + \frac{\alpha_s}{2\pi} C_F \left\{ \frac{\pi^2}{v} - 6 + \pi^2 v + \mathcal{O}() \right\} \right]. \tag{10}$$

Although non-perturbative resonance effects at threshold supersede predictions made by perturbation theory, Eq. (10) gives essential information on σ_F sufficiently above the production resonance.

Combining Eqs. (9) and (10) yields the following Schwinger representation for σ_F

$$\frac{\sigma_{F/1}}{\sigma_{F/0}} = 1 + C_F \, \alpha_s \, \frac{\pi}{2} \left(\frac{1}{v} - \varphi(v) \right), \tag{11}$$

with the mass-zero condition $\varphi(1) \equiv 1$. This mass-zero condition is an absolute requirement for any φ-representation, whereas the exact threshold value $\varphi(0) = 6/\pi^2$ is of lesser importance due to the $1/v$-pole dominance in Eq. (11). In general, $\varphi(v)$ is a function of $0 \le v \le 1$ and contains apart from the universal term in Eq. (11) (describing the color interaction of the quarks close to threshold) all the non-trivial energy dependence of $\sigma_{F/1}$. Suitable φ-representations that provide excellent approximations to the exact solutions are simple polynomials of degree $m \ge 2$:

$$\varphi_m(v) = \frac{\sum\limits_{i=0}^{m} a_i \, v^i}{\sum\limits_{i=0}^{m} a_i}. \tag{12}$$

Tab. 1 displays the coefficients a_i for the lowest-order representations φ_2, φ_3, and φ_4. In Fig. 1, we have plotted these polynomial representations together with the exact result. Already the second-order form φ_2 gives a very accurate interpolation so that the

[†] Note the typographical error in Table I of Ref. [11]. The correct limiting behavior of the 'spin-dependent' integral $\tilde{\mathcal{S}}_5$ close to threshold ($v \to 0$) is $\tilde{\mathcal{S}}_5 \sim 4\big(\,2 \ln v - 1\,\big) + \mathcal{O}()$.

corresponding Schwinger formula Eq. (11) provides a very compact expression for easy implemention of the $\mathcal{O}(\alpha)$ corrections to $\sigma_{_F}$.

A straightforward procedure to include these massive $\mathcal{O}(\alpha)$ effects already in the Born approximation consists in the introduction of effective couplings. From Eqs.(3) and (11) we obtain directly the prescription

$$g^{VA} \;\rightarrow\; \tilde{g}^{VA} = g^{VA}\,\left[\,1 + C_{_F}\,\alpha_s\,\frac{\pi}{2}\left(\,\frac{1}{v} - \varphi_m(v)\,\right)\,\right], \tag{13}$$

where $\varphi_m(v)$ are the appropriate polynomials of Tab. 1.

Similarly, one finds replacements rules for the two remaining couplings, g^{VV} and g^{AA}, that multiply with the $\mathcal{C}$-even components of the differential rate. They contribute through the VV and AA parity-parity combinations of the intermediate γ, Z states to the to the total rate

$$\sigma_{_T} = \frac{4\pi\alpha^2}{q^2}\;\left[\,\tfrac{1}{2}v\,(3-v^2)\,g^{VV} + v^3 g^{AA}\,\right]. \tag{14}$$

Using the third-order Schwinger represention given in Ref. [11], we find the following explicit $\mathcal{O}(\alpha)$ expressions

$$\begin{aligned}\tilde{g}^{VV} \;&=\; \left[\,Q_q^2 - 2\,Q_q v_e v_q\,\mathrm{Re}\,\chi_{_Z} + (v_e^2+a_e^2)\,v_q^2\,|\chi_{_Z}|^2\,\right]\;\times \\ &\quad\left[\,1 + C_{_F}\,\alpha_s\left\{\frac{\pi}{2v} - \left(\frac{\pi}{2} - \frac{3}{4\pi}\right)\frac{95 - 82v + 173v^2 - 85v^3}{101}\right\}\right],\end{aligned} \tag{15}$$

and

$$\begin{aligned}\tilde{g}^{AA} \;&=\; (v_e^2+a_e^2)\,a_q^2\,|\chi_{_Z}|^2\;\times \\ &\quad\left[\,1 + C_{_F}\,\alpha_s\left\{\frac{\pi}{2v} - \left(\frac{\pi}{2} - \frac{3}{4\pi}\right)\frac{43 - 30v + 15v^2 + 71v^3}{99}\right\}\right].\end{aligned} \tag{16}$$

Now all ingredients are available to treat the forward-backward asymmetries of heavy quarks at QCD one-loop level. The forward backward-asymmetry $A_{_{FB}}^f$ measures the fermion events in the forward and backward hemispheres and is therefore defined as

$$A_{_{FB}}^f \;=\; \frac{\displaystyle\int_0^1 d\cos\theta\;\frac{d\,\sigma}{d\cos\theta} - \int_{-1}^0 d\cos\theta\;\frac{d\,\sigma}{d\cos\theta}}{\displaystyle\int_0^1 d\cos\theta\;\frac{d\,\sigma}{d\cos\theta} + \int_{-1}^0 d\cos\theta\;\frac{d\,\sigma}{d\cos\theta}}\;, \tag{17}$$

which immediately gives with Eq. (1)

$$A_{FB}^{f} \;=\; \frac{3}{4}\,\frac{\sigma_F}{\sigma_U+\sigma_L}. \tag{18}$$

For heavy-quark production, the $\mathcal{O}(\alpha)$ corrections for A_{FB}^{q} take a particularly simple form when expressed in terms of the effective couplings $\tilde{g}^{ij}$, with $i,j = V,A$. Using Eqs. (2) and (14) we obtain

$$A_{FB/1}^{q} = \frac{3v\,\tilde{g}^{VA}}{(3-v^2)\,\tilde{g}^{VV}+2v^2\tilde{g}^{AA}}. \tag{19}$$

Close to the Z-peak, the $|\chi_Z|^2$ propagator terms in the couplings dominate and the corresponding Born expression $A_{FB/0}^{q}$ reduces to the approximate formula given in Ref. [12].

Fig. 2 shows the energy dependence of A_{FB}^{q} for charm, bottom, and top quark in the Born approximation (solid line) and including the $\mathcal{O}(\alpha)$ final state corrections (dashed line). For the running of the strong coupling we have used the central value $\alpha_s^{(5)}(M_Z) = 0.118$ with five active flavors on the Z-peak. Crossing the top-quark threshold the appropriate matching condition has to be imposed. For charm and bottom quark, the fixed-point masses $m_c(m_c) = 1.3$ GeV and $m_b(m_b) = 4.33$ GeV correspond to $m_c(M_Z) = 0.78$ GeV and $m_b(M_Z) = 3.20$ GeV, respectively. In the top-quark case, we have chosen $M_t = 180$ GeV as pole mass, which gives the fixed-point mass $m_t(m_t) = 172.1$ GeV. In each individual plot of Fig. 2, the dashed-dotted line refers to the right-hand scale measuring the absolute difference between Born and $\mathcal{O}(\alpha)$ predictions, *i.e.* $\Delta A_{FB}^{q} = A_{FB/1}^{q} - A_{FB/0}^{q}$. For certain center-of-momentum energies a subtle cancellation of the $\mathcal{O}(\alpha)$ expressions in the numerator and denominator of Eq. (18) takes place and gives dynamical zeros for ΔA_{FB}^{q}.

Fig. 2(a) highlights the two specific energy values $E_{cms} = 6.58$ GeV and $E_{cms} = 89.362$ GeV at which the massive one-loop QCD corrections vanish. At the first energy point, we find $A_{FB/0}^{c}(6.58\text{ GeV}) = A_{FB/1}^{c}(6.58\text{ GeV}) = 0.0038$. Of particular interest is the energy domain close to 89.362 GeV, where both lowest-order as well as $\mathcal{O}(\alpha)$ one-loop contributions to the forward-backward asymmetry vanish. These cancellations originate from the dynamical interplay of the involved electroweak couplings at Born level. Note that the $\mathcal{O}(\alpha)$ result factorizes with the Born term so that the isolated one-loop zero occurs only for the lower energy value $E_{cms} = 6.58$ GeV.

As illustrated in Fig. 2(b), a similar situation arises for the bottom quark. Here, our theoretical predictions for the dynamical zeros are $A^b_{FB/0}(23.32\ \mathrm{GeV}) = -0.1015$ with $\Delta A^b_{FB}(23.32\ \mathrm{GeV}) = 0$, and $A^b_{FB/0}(85.235\ \mathrm{GeV}) = A^b_{FB/1}(85.235\ \mathrm{GeV}) = 0$.

An interesting observation is that for charm and bottom quark the lower energy values yielding dynamical zeros correspond both to approximately the same mass scale $v = 0.9512$. Note that on the Z-peak the predictions of Figs. 2(a) and (b) agree very well with the recent estimates of Ref. [12].

Due to the high production threshold of the top quark, only one first-order α_s zero is located at 848.80 GeV in Fig. 2(c). The corresponding forward-backward asymmetry at Born level is $A^t_{FB/0} = 0.5557$.

To isolate the energy dependence of the non-trivial one-loop contents in $A^q_{FB/1}$, we introduce the function $\Phi^q(v)$ in the following manner

$$A^q_{FB/1} = A^q_{FB/0} \left[1 + \frac{\alpha_s}{\pi} \Phi^q(v) \right]. \tag{20}$$

Note that $\Phi^q(v)$ contains additional couplings g^{VV} and g^{AA}, which depend solely on v once the quark type q is fixed and the corresponding running mass $m_q(q^2)$ is implemented.

In the following, we shall use the notation Φ^q for the exact $\mathcal{O}(\alpha)$ result derived from the analytic expressions for σ_F and σ_T as given in Eq. (5) and in Ref. [11], respectively. Any additional subscript will indicate approximate representations different from the exact formula Φ^q.

The exact result Φ^q involves all the analytic integral solutions listed in Ref. [6] yielding complicated and lengthy expressions. However, using simple polynomial interpolations for the couplings $\tilde{g}^{ij}$, we can obtain compact and very accurate approximations that allow for an easy implementation of the forward-backward asymmetry. For example, the substitution of the $\mathcal{O}()$ expressions Eqs. (13), (15), and (16)) into Eq. (19) gives such a useful representation, which we denote as Φ^q_3.

Further simplification is accomplished by expanding numerator and denominator of Eq. (19) up to first oder in α_s. After inserting the numerical values for the relevant electroweak couplings and the running of the quark masses, we find the following lowest-

order (L) interpolations

$$\Phi_{_L}^{b,c}(v) = -191.175 + 413.338\,v - 223.098\,v^2, \tag{21}$$

$$\Phi_{_L}^{t}(v) = -0.427 + 5.187\,v - 5.070\,v^2. \tag{22}$$

Note that in this representation $\Phi_{_L}$ is practically insensitive to the distinct couplings and masses of bottom and charm quark, *i.e.* $\Phi_{_L}^{b,c}(1) \approx -1$. Only the top quark requires a separate parametrization due to its exceptionally high mass.

To illustrate the high accuracy of these compact formulas, we have plotted in Figs. 3 the representations Φ_3 and $\Phi_{_L}$, and the exact $\mathcal{O}(\alpha)$ result Φ for charm, bottom, and top quark. Furthermore, we have also included the following approximation obtained from an expansion of the form factors to second order in $\sqrt{\xi}$ (first order in m) as given in Ref. [5]

$$\Phi_{_Z}^{q} = -1 + \tfrac{8}{3}\sqrt{\xi} + \tfrac{1}{3}\xi\left[7 + \tfrac{1}{6}\pi^2 - 2\ln\left(\tfrac{1}{2}\sqrt{\xi}\right) + \ln^2\left(\tfrac{1}{2}\sqrt{\xi}\right)\right] - 3\,\xi\,\frac{v_q^2 - 2a_q^2\ln\left(\frac{1}{2}\sqrt{\xi}\right)}{v_q^2 + a_q^2}. \tag{23}$$

Note that $\Phi_{_Z}$ contains a part which explicitly depends on the electroweak couplings. This formula has primarily been used for approximate estimates on the Z-peak.

Comparing Figs. 3(a) and (b), we recognize that in the charm- and bottom-quark case for $v > 0.8$ all specific properties as flavor and mass effects fully factorize with the Born contribution $A_{FB/0}^{c,b}$, and Φ exhibits the same universal functional dependence. In the region $v > 0.9$, which corresponds to center-of-momentum energies above 5 and 20 GeV for charm and bottom quark, respectively, $\Phi_{_L}$ gives the best representation. Closer to threshold, Φ_3 provides more accurate numerical estimates.

Fig. 3(c) demonstrates that for the top quark $\Phi_{_L}$ and Φ_3 yield far better results than $\Phi_{_Z}$. Higher-order mass terms in $\Phi_{_Z}$ should be taken into account to reach a comparable precision.

To complete this discussion, we present in Tabs. 2–4 the explicit numerical values of Born and $\mathcal{O}(\alpha)$ contributions to the forward-backward asymmetry for charm, bottom, and top quark with the same choice for $\alpha_s(M_{_Z})$ and the fixed-point quark masses $m_q(m_q)$ as in Fig. 2. In the fourth column the impact of the $\mathcal{O}(\alpha)$ contributions on the Born result is given by $(A_{FB/1}^q - A_{FB/0}^q)/A_{FB/0}^q$ in percent. Again, $A_{FB/3}^q$, $A_{FB/L}^q$, and $A_{FB/Z}^q$ denote the estimates stemming from Φ_3^q, $\Phi_{_L}^q$, and $\Phi_{_L}^q$, respectively. For these approximate

results we also provide in the adjacent columns the relative error to $A^q_{FB/1}$ in percent. By comparing these relative errors with the corresponding percentages capturing the exact $\mathcal{O}(\alpha)$ modifications, one obtains a reliable measure of the quality of the approximations.

In this work, we have investigated the QCD one-loop corrections to the single-jet forward-backward asymmetries for massive quarks off the Z-resonance, which modify the Born predictions by approximately 3%. After finding compact Schwinger representations for the $\mathcal{C}$-odd contribution in the angular distribution of the produced quark, we derived simple polynomial expressions that provide excellent approximations for the $\mathcal{O}(\alpha)$ forward-backward asymmetry.

Due to a dynamical cancellation of $\mathcal{C}$-even and $\mathcal{C}$-odd components in the single-jet asymmetry, $\mathcal{O}(\alpha)$ zeros occur close to the Z-peak at 89.362 GeV for charm production and at 85.235 GeV for bottom production. A thorough experimental investigation of this effect should reveal interesting new insights in the physics at higher-order QCD level and might even allow for a detection of signals beyond the Standard Model.

Acknowledgements. It is a pleasure to thank J. Bernabéu and J. Peñarrocha for a critical reading of the manuscript, and K. Kleinknecht for a helpful conversation. I further acknowledge the support given by the Alexander-von-Humboldt Foundation and CICYT under grant AEN93-0234.

References

[1] The ALEPH Collaboration, D. Busculic *et al.*, Phys. Lett. B **352**, 479 (1995), and Z. Phys. C **62**, 179 (1994).

[2] The DELPHI Collaboration, P. Abreu *et al.*, Z. Phys. C **66**, 341 (1995).

[3] The OPAL Collaboration, G. Alexander *et al.*, *Measurement of the Heavy Quark Forward-Backward Asymmetries and Average B Mixing Using Leptons in Multi-Hadronic Events*, CERN Report No. CERN-PPE/95-179, December 1995 (unpublished), and R. Akers *et al.*, Z. Phys. C **68**, 203 (1995).

[4] A. Djouadi, J.H. Kühn, and P.M. Zerwas, Z. Phys. C **46**, 411 (1990).

[5] J.B. Stav and H.A. Olsen, Phys. Rev. D **52**, 1359 (1995).

[6] M.M. Tung, J. Bernabéu, and J. Peñarrocha, *Analytic* $\mathcal{O}(\alpha)$ *Results for Bottom and Top Quark Production in* e^+e^- *Collisions*, preprint no. FTUV/95-38 and IFIC/95-40, November 1995 (hep-ph/9601277).

[7] J.G. Körner, A. Pilaftsis and M.M. Tung, Z. Phys. C **63**, 575 (1994) (hep-ph/9311332); M.M. Tung, Ph.D. thesis, University of Mainz, 1993.

[8] J. Jeršak, E. Laermann and P.M. Zerwas, Phys. Lett. B **98**, 363 (1981); Phys. Rev. D **25** 1218 (1982).

[9] J.G. Körner and M.M. Tung, Z. Phys. C **64**, 255 (1994).

[10] J. Schwinger, *Particles, Sources and Fields* (Addison-Wesley, Redwood City, 1988), Vol. III, pp. 99.

[11] M.M. Tung, Phys. Rev. D **52**, 1353 (1995) (hep-ph/9403322).

[12] A. Djouadi, B. Lampe, and P.M. Zerwas, Z. Phys. C **67**, 123 (1995) (hep-ph/9411386).

Figure Captions

Fig. 1: Schwinger representations for the QCD one-loop corrections to $\sigma_{_F}$ in the differential rate of the production process $e^+e^- \to \gamma, Z \to q\bar{q}(g)$. The exact result is compared to the polynomial representations of degree $m = 2, 3$, and 4.

Fig. 2: The single-jet forward-backward asymmetry $A^q_{_{FB}}$ in the Born approximation and at $\mathcal{O}(\alpha)$ as a function of the center-of-momentum energy for (a) charm, (b) bottom, and (c) top production. The dashed-dotted line refers to the right ordinate where $\Delta A^q_{_{FB}}$ denotes the difference between Born and $\mathcal{O}(\alpha)$ results.

Fig. 3: Non-trivial one-loop contents of $A^q_{_{FB/1}}$ as a function of $v = \sqrt{1 - 4m_q^2/q^2}$ for (a) charm, (b) bottom, and (c) top quark. The exact result Φ^q is compared to the representations $\Phi_{_3}$, $\Phi_{_L}$, and $\Phi_{_Z}$.

Table Captions

Tab. 1: Coefficients for the lowest-order Schwinger representations of $\sigma_{_F}$.

Tab. 2: Forward-backward asymmetry for $e^+e^- \to \gamma, Z \to c\bar{c}$ at Born level and up to $\mathcal{O}(\alpha)$ compared to estimates given by Φ_3, $\Phi_{_L}$, and $\Phi_{_Z}$ ($\alpha_s(M_{_Z}) = 0.118$ and $m_c(m_c) = 1.3$ GeV).

Tab. 3: Forward-backward asymmetry for $e^+e^- \to \gamma, Z \to b\bar{b}$ at Born level and up to $\mathcal{O}(\alpha)$ compared to estimates given by Φ_3, $\Phi_{_L}$, and $\Phi_{_Z}$ ($m_b(m_b) = 4.33$ GeV).

Tab. 4: Forward-backward asymmetry for $e^+e^- \to \gamma, Z \to t\bar{t}$ at Born level and up to $\mathcal{O}(\alpha)$ compared to estimates given by Φ_3, $\Phi_{_L}$, and $\Phi_{_Z}$ ($M_t = 180$ GeV).

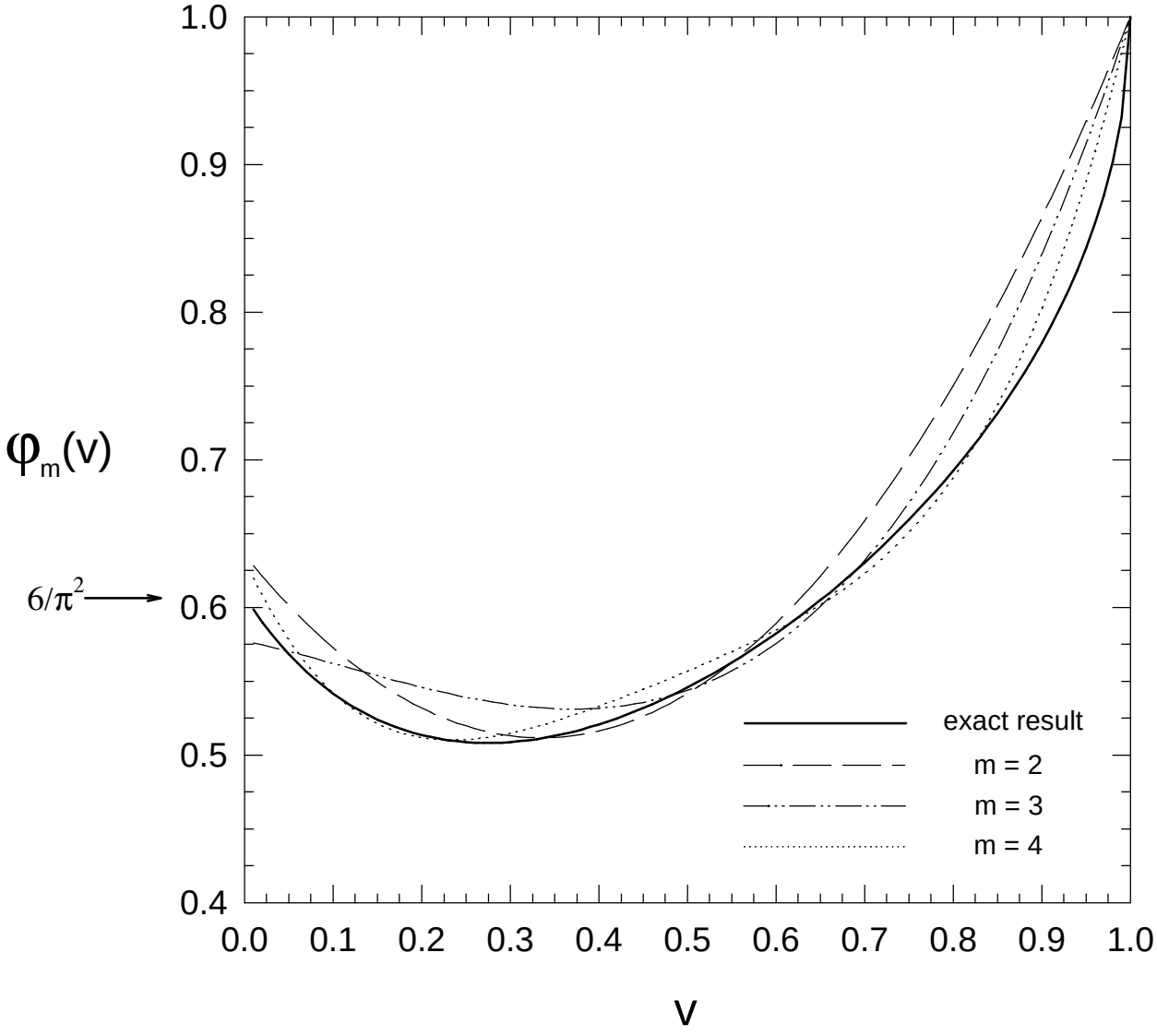
1.0
0.9
0.8
0.7
0.6
0.5
0.4
$\varphi_m(v)$
$6/\pi^2$
0.0
0.1
0.2
0.3
0.4
0.5
0.6
0.7
0.8
0.9
1.0
v
exact result
m = 2
m = 3
m = 4

Figure 1

$\varphi_m(v)$	a_0	a_1	a_2	a_3	a_4
$m=2$	61	-71	106	—	—
$m=3$	56	-13	-28	82	—
$m=4$	62	-129	463	-641	343

Table 1

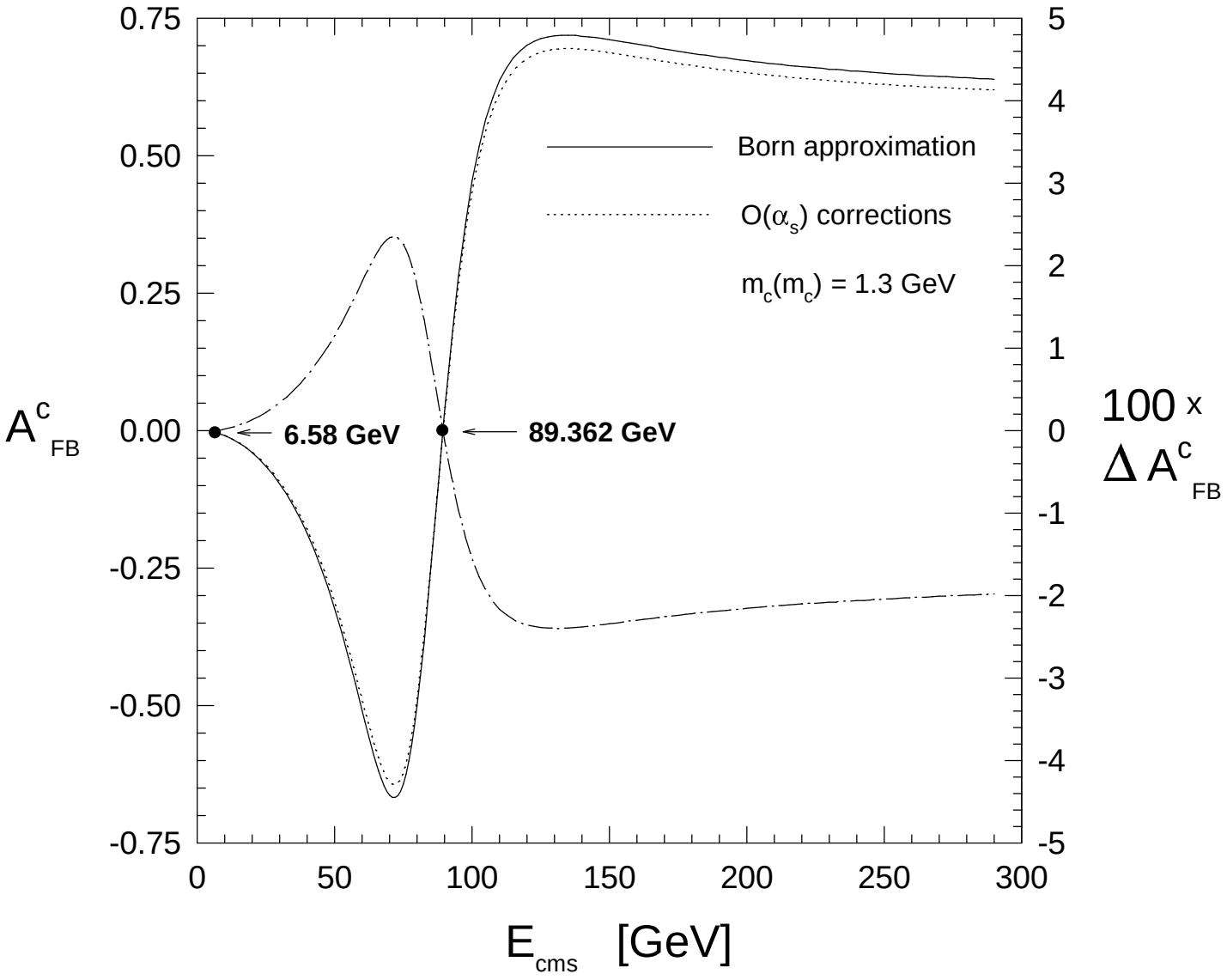
0.75
0.50
0.25
0.00
-0.25
-0.50
-0.75
5
4
3
2
1
0
-1
-2
-3
-4
-5
0
50
100
150
200
250
300
Born approximation
O(α_s) corrections
m_c(m_c) = 1.3 GeV
6.58 GeV
89.362 GeV
A^c_FB
100 x Δ A^c_FB
E_cms [GeV]

Figure 2(a)

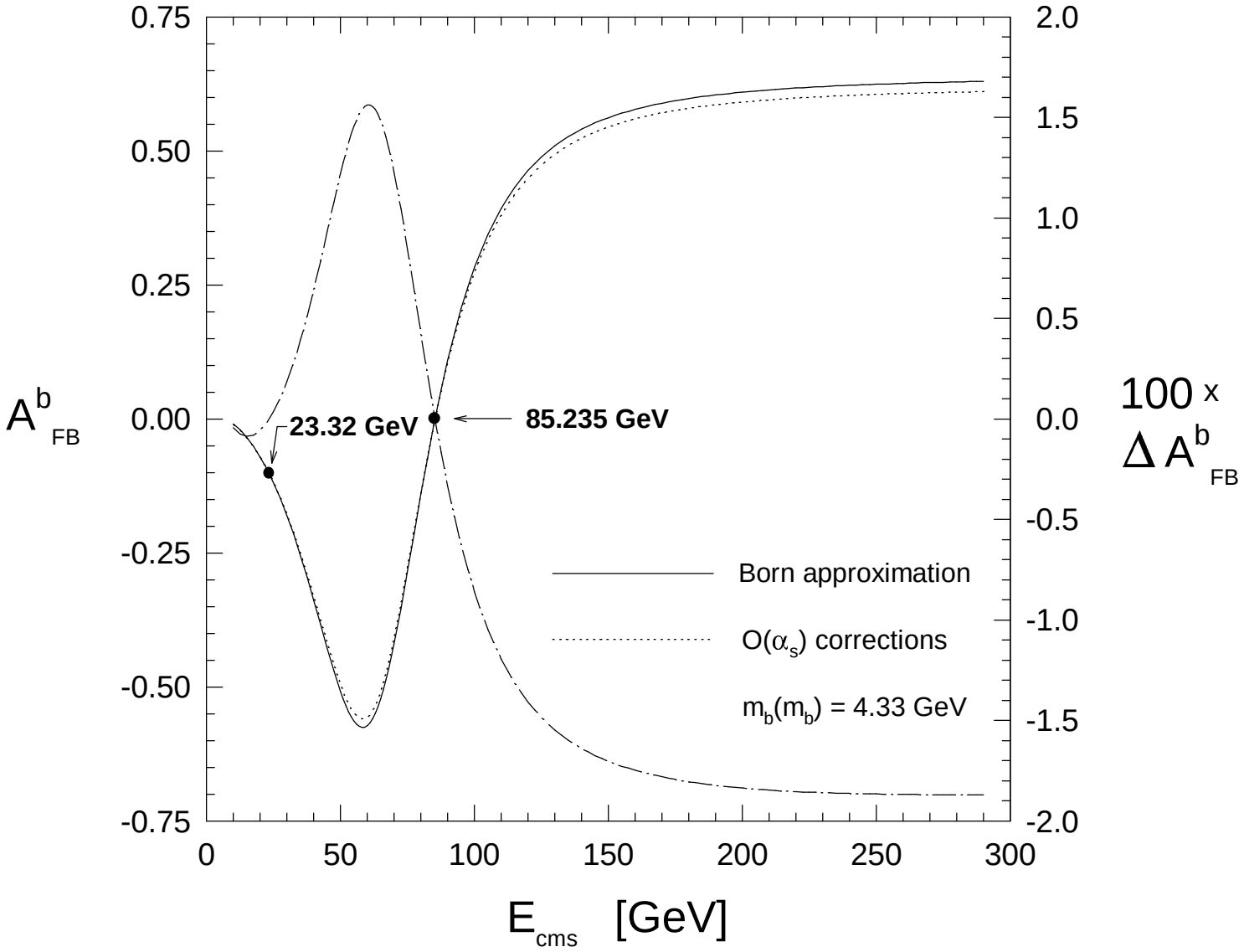
0.75
0.50
0.25
0.00
-0.25
-0.50
-0.75
2.0
1.5
1.0
0.5
0.0
-0.5
-1.0
-1.5
-2.0
0
50
100
150
200
250
300
A^b_{FB}
$100 \times \Delta A^b_{FB}$
E_{cms} [GeV]
23.32 GeV
85.235 GeV
Born approximation
$O(\alpha_s)$ corrections
$m_b(m_b) = 4.33$ GeV

Figure 2(b)

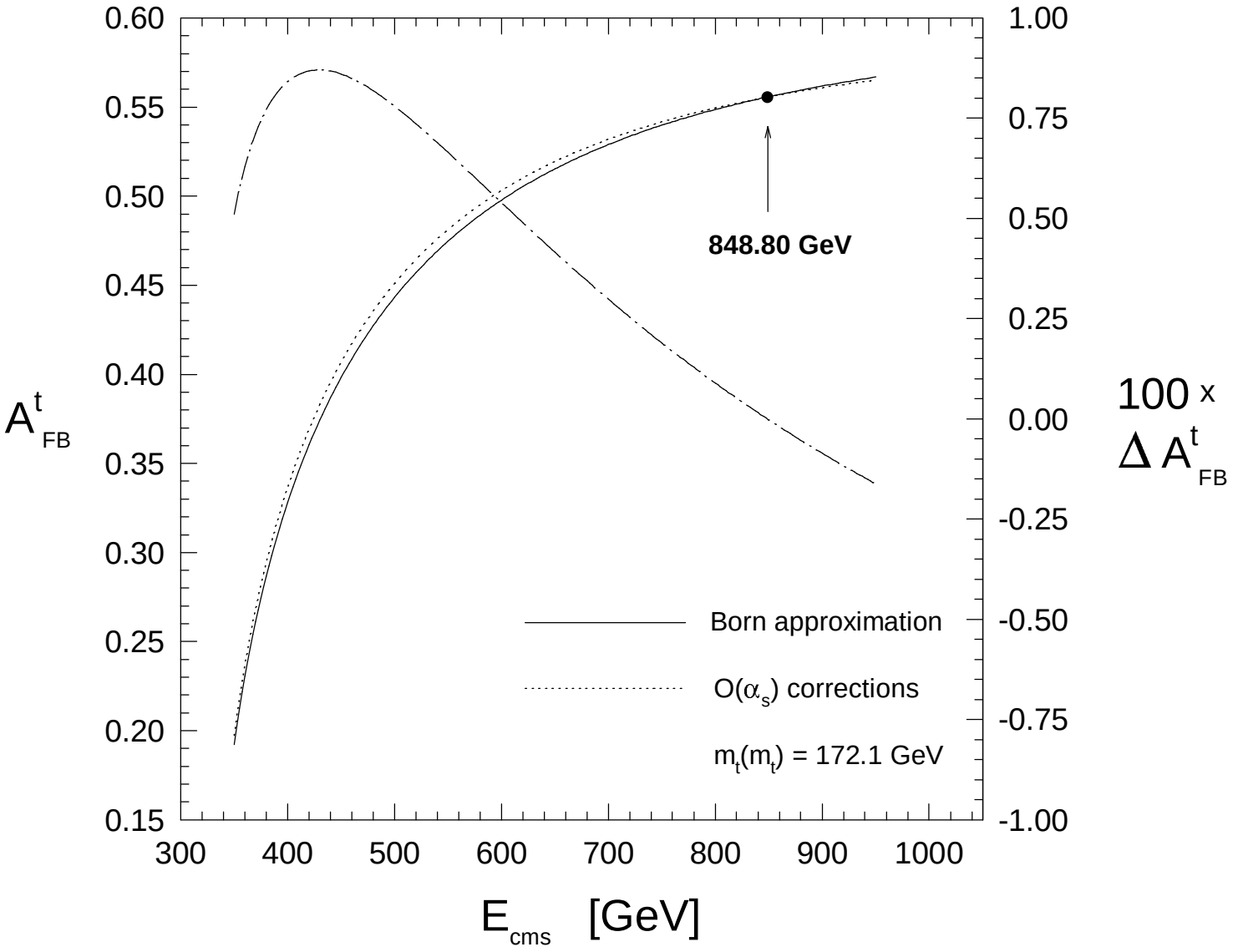
0.60
0.55
0.50
0.45
0.40
0.35
0.30
0.25
0.20
0.15
1.00
0.75
0.50
0.25
0.00
-0.25
-0.50
-0.75
-1.00
300
400
500
600
700
800
900
1000
A^t_{FB}
$100 \times \Delta A^t_{FB}$
E_{cms} [GeV]
848.80 GeV
Born approximation
$O(\alpha_s)$ corrections
$m_t(m_t)$ = 172.1 GeV

Figure 2(c)

E_{cms}	$A^c_{FB/0}$	$A^c_{FB/1}$	%	$A^c_{FB/3}$	%	$A^c_{FB/L}$	%	$A^c_{FB/Z}$	%
5	-0.00202	-0.00206	1.94	-0.00201	2.48	-0.00205	0.62	-0.00195	5.36
6.58	-0.00382	-0.00382	0	-0.00372	2.73	-0.00385	-0.79	-0.00368	3.84
7	-0.00439	-0.00437	-0.36	-0.00425	2.70	-0.00440	-0.65	-0.00422	3.52
10	-0.00943	-0.00924	-1.95	-0.00904	2.20	-0.00922	0.26	-0.00905	2.05
50	-0.32444	-0.31285	-3.57	-0.31170	0.37	-0.31220	0.21	-0.31212	0.23
75	-0.64299	-0.62039	-3.51	-0.61910	0.21	-0.61993	0.07	-0.61942	0.16
85	-0.24940	-0.24071	-3.49	-0.24029	0.17	-0.24061	0.04	-0.24037	0.14
89.362	$-9.98\cdot10^{-6}$	$-9.64\cdot10^{-6}$	-3.47	$-9.62\cdot10^{-6}$	0.16	$-9.63\cdot10^{-6}$	0.03	$-9.62\cdot10^{-6}$	0.14
90	0.03516	0.03394	-3.47	0.03389	0.16	0.03393	0.03	0.03390	0.14
91.187	0.09807	0.09467	-3.47	0.09452	0.16	0.09464	0.03	0.09454	0.14
92	0.14015	0.13529	-3.46	0.13508	0.16	0.13525	0.03	0.13511	0.14
100	0.45361	0.43804	-3.43	0.43740	0.14	0.43795	0.02	0.43745	0.13
250	0.65009	0.62969	-3.14	0.62937	0.05	0.63008	-0.06	0.62900	0.11
500	0.61853	0.60036	-2.94	0.60023	0.02	0.60089	-0.09	0.59981	0.09

Table 2

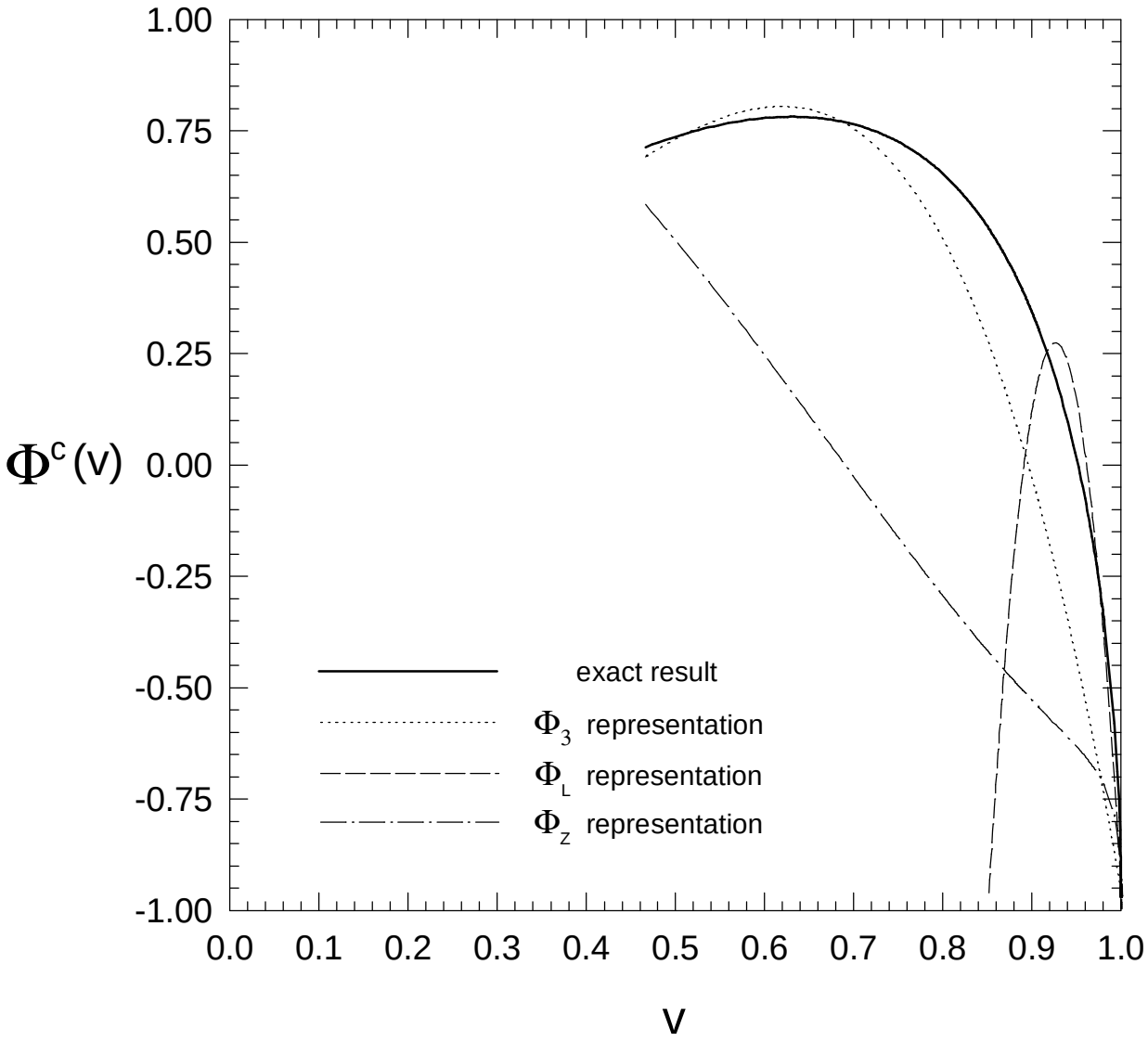
1.00
0.75
0.50
0.25
0.00
-0.25
-0.50
-0.75
-1.00
0.0
0.1
0.2
0.3
0.4
0.5
0.6
0.7
0.8
0.9
1.0
v
Φc (v)
exact result
Φ3 representation
ΦL representation
ΦZ representation

Figure 3(a)

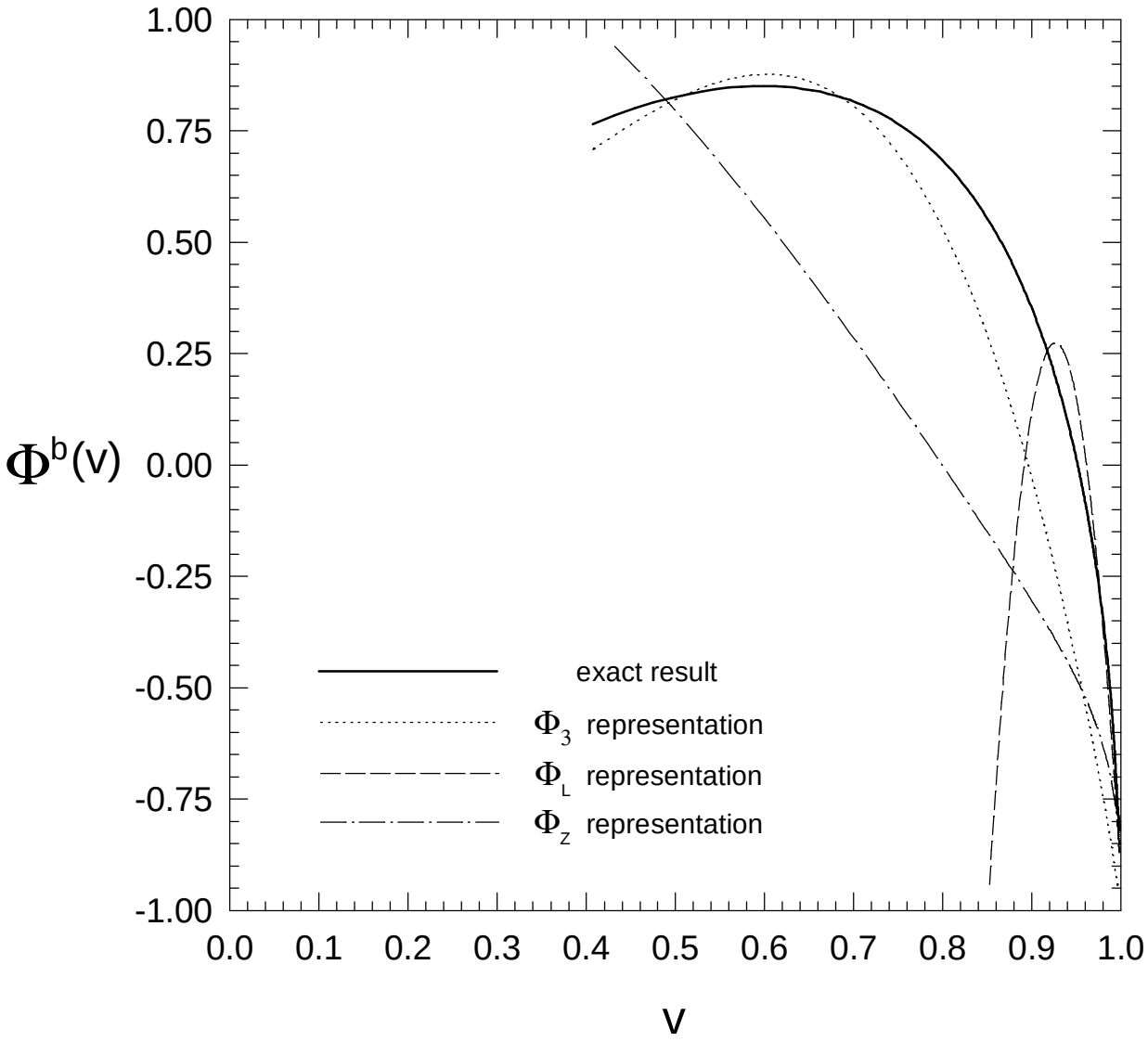
1.00
0.75
0.50
0.25
0.00
-0.25
-0.50
-0.75
-1.00
0.0
0.1
0.2
0.3
0.4
0.5
0.6
0.7
0.8
0.9
1.0
v
Φ^b(v)
exact result
Φ_3 representation
Φ_L representation
Φ_Z representation

Figure 3(b)

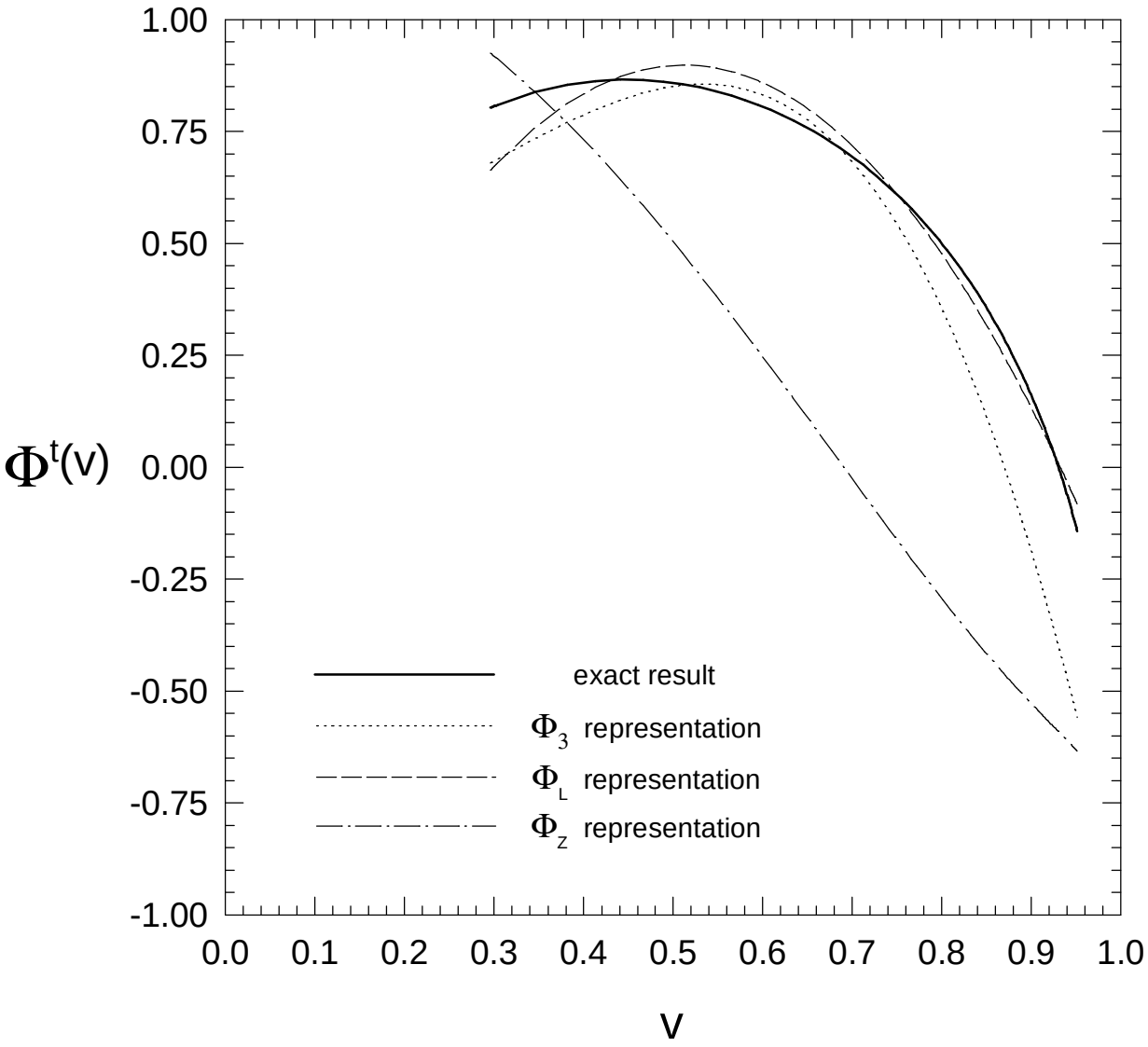
1.00
0.75
0.50
0.25
0.00
-0.25
-0.50
-0.75
-1.00
0.0
0.1
0.2
0.3
0.4
0.5
0.6
0.7
0.8
0.9
1.0
v
Φ^t(v)
exact result
Φ_3 representation
Φ_L representation
Φ_Z representation

Figure 3(c)

E_{cms}	$A^b_{FB/0}$	$A^b_{FB/1}$	%	$A^b_{FB/3}$	%	$A^b_{FB/L}$	%	$A^b_{FB/Z}$	%
20	-0.07066	-0.07122	0.78	-0.06972	2.10	-0.07158	-0.51	-0.06927	2.73
23.32	-0.10138	-0.10137	0	-0.09920	2.14	-0.10201	-0.63	-0.09908	2.27
25	-0.11903	-0.11865	-0.32	-0.11614	2.11	-0.11927	-0.53	-0.11620	2.07
50	-0.50841	-0.49620	-2.40	-0.49011	1.23	-0.49470	0.30	-0.49320	0.60
75	-0.28405	-0.27560	-2.98	-0.27368	0.69	-0.27511	0.18	-0.27517	0.15
80	-0.14017	-0.13595	-3.01	-0.13508	0.64	-0.13572	0.17	-0.13577	0.13
85	-0.00589	-0.00571	-3.03	-0.00568	0.60	-0.00570	0.18	-0.00570	0.13
85.235	$6.048{\cdot}10^{-6}$	$5.865{\cdot}10^{-6}$	-3.03	$5.829{\cdot}10^{-6}$	0.60	$5.854{\cdot}10^{-6}$	0.18	$5.857{\cdot}10^{-6}$	0.13
90	0.11003	0.10669	-3.03	0.10608	0.57	0.10650	0.18	0.10656	0.12
91.178	0.13436	0.13029	-3.04	0.12955	0.56	0.13005	0.18	0.13012	0.12
95	0.20568	0.19943	-3.04	0.19835	0.54	0.19906	0.19	0.19918	0.13
100	0.28275	0.27415	-3.04	0.27274	0.52	0.27364	0.19	0.27380	0.13
250	0.62459	0.60593	-2.99	0.60472	0.20	0.60554	0.06	0.60525	0.11
500	0.63795	0.61964	-2.87	0.61908	0.09	0.61979	-0.02	0.61906	0.09

Table 3

E_{cms}	$A^t_{FB/0}$	$A^t_{FB/1}$	%	$A^t_{FB/3}$	%	$A^t_{FB/L}$	%	$A^t_{FB/Z}$	%
350	0.19218	0.19729	2.66	0.19665	0.32	0.19681	0.24	0.19729	$-2{\cdot}10^{-3}$
500	0.44327	0.45107	1.76	0.44986	0.27	0.45097	0.02	0.44050	2.34
750	0.53985	0.54174	0.35	0.53599	1.06	0.54143	0.06	0.53124	1.94
800	0.54862	0.54952	0.16	0.54338	1.12	0.54942	0.02	0.53953	1.82
845	0.55516	0.55523	0.01	0.54884	1.15	0.55536	-0.02	0.54572	1.71
848.8	0.55566	0.55566	0	0.54925	1.15	0.55581	-0.03	0.54619	1.70
850	0.55582	0.55580	0	0.54939	1.15	0.55596	-0.03	0.54634	1.70
1000	0.57106	0.56874	-0.41	0.56199	1.19	0.56974	-0.17	0.56077	1.40

Table 4